Modeling Three-Dimensional Avascular Tumor Growth Using Lattice Gas Cellular Automata

Sachin Man Bajimaya Shrestha, Grand Joldes, Adam Wittek, and Karol Miller

Abstract We model and simulate avascular tumor growth in three dimensions using lattice gas cellular automata (LGCA). Our 3D models are an advance over current state-of-the-art where most three dimensional (3D) models are in fact only a series of two dimensional models simulated to give an appearance of a 3D model. In our 3D model, we use binary description of cells and their states for computational speed and efficiency. The fate and distribution of cells in our model are determined by the Lattice–Boltzmann energy. We simulate our model in a comparable size of lattice and show that the findings are in good agreement with biological tumor behavior.

Keywords Tumor growth • Heterogeneous tumor • Three-dimensional model • Lattice gas cellular automata

1 Introduction

The fact that one person out of three will be treated for some form of cancer in their lifetime [1] has motivated many studies into cancer over the past several decades. However, so far, neither incidence nor mortality of human cancer has been much diminished by conscious human intervention. A better understanding of the cellular basis underlying tumor growth may eventually open the door to its successful treatment, as will the development of novel drugs and therapies based on the results of molecular and cellular biological cancer research. It is hoped that a three dimensional (3D) model of tumor and its simulation will prove to be a milestone in this quest as such models are more representative of a tumor in vivo.

S.M.B. Shrestha • G. Joldes • A. Wittek • K. Miller (✉)
Intelligent Systems for Medicine Laboratory,
The University of Western Australia, Crawley, WA 6009, Australia
e-mail: karol.miller@uwa.edu.au

B. Doyle et al. (eds.), *Computational Biomechanics for Medicine: Fundamental Science and Patient-specific Applications*, DOI 10.1007/978-1-4939-0745-8_2,

The avascular growth phase of tumor is also called the primary growth phase. Growth of tumor in this phase depends on the supply of nutrients and its size is limited by the diffusion of these nutrients. Tumors in the avascular phase are considered relatively benign, and the detection and treatment of tumors at this stage provide a greater probability of having the disease cured.

In our earlier work [2], we modeled and simulated avascular tumor growth in two dimensions. The model incorporated a heterogeneous population of cells—proliferating, quiescent, necrotic, apoptotic, and mutated cells. Mutation of cells gives rise to cells of a different phenotype that have the ability to survive at lower levels of nutrient concentration and reproduce faster. The concentration of nutrients available for each cell in the tumor volume is decided by solving the diffusion equation. Although the model was able to capture the tumor growth dynamics at the cellular level, simulation of large size of tumor was not possible due to the computational burden of solving the diffusion equation.

In our most recent work [3], we modeled the complete growth of an avascular tumor by employing cellular automata for the growth of cells and a steady-state equation to solve for nutrient concentrations. Through simulation, we showed that, in the case of a brain tumor, oxygen distribution in the tumor volume may be sufficiently described by a time-independent steady-state equation without losing the characteristics of a time-dependent diffusion equation. This made the solution of oxygen concentration in the tumor volume computationally more efficient, thus enabling simulation of tumor growth on a large scale. The results from our growth simulation compared well with existing experimental data on Ehrlich ascites carcinoma and tumor spheroid cultures. Nonetheless, a 3D model of tumor would serve a better purpose of investigating tumor growth dynamics due to its similarity with a tumor in vivo. However, the growth simulation of the model obtained by extending our model into 3D was unattainable due to excessive computational burden. Given that the two dimensional (2D) simulation of the complete growth of tumor using this approach required about 18 h on average to complete on a desktop computer with a 3.2 GHz processor and 12 GB of RAM [3], it can be estimated that a 3D computation of the tumor growth to a similar size would take at least 10 days on a computer with the same specifications. A similar problem arose with an implementation of the 3D model on Graphics Processing Units (GPUs) for general purpose computations due to insufficient internal memory to hold the complete data.

Therefore, a majority of research in the area of tumor growth modeling is limited to pattern formation in a growing tumor [4–6] due to either the inherent time-consuming nature of numerical solution to partial differential equations or simulating growth on a macro-scale starting from a few cells is computationally very expensive.

In [7], a simulation of an early 3D model is presented. However, details of the method used for the development of their model are not presented. Their model does not include tumor heterogeneity. More importantly, the tumor resulting from the simulation of their model contains less than 1,000 cells, and therefore, the size of tumor is too small for any practical studies.

In [8], a 3D tumor model is developed using the finite element approach and is based on governing equations obtained via the thermodynamically constrained averaging theory. We have presented the limitations of the continuum approach of modeling tumor growth, the behavior of which is governed by the discrete state of each of its constituent cells, in our earlier work [3].

Another work in the development of a 3D model may be found in [9] where part of the secondary phase of tumor growth is modeled. Specifically, the development of vasculature inside the tumor is modeled using a hybrid discrete-continuum approach.

Most existing literature pass on the idea of developing a 3D model by suggesting that extending a 2D model into 3D is obvious and simple; and some leave it for future work. At their best, some present 3D models of tumor that are a series of 2D models simulated to give an appearance of a 3D model.

In this paper, we present the Lattice Gas Cellular Automata (LGCA) model of the 3D growth of tumor. We use the binary description of cells and their states in our model for computational speed and efficiency. The fate and distribution of cells in our model are determined by the Lattice–Boltzmann Energy [10].

In the rest of this paper, we present, in order, the basics of LGCA, the transition rules, the formation of our 3D tumor growth model including the interaction and the transport steps, and finally, the results and discussion.

2 Lattice Gas Cellular Automata

The LGCA model was introduced by Hardy, de Passis, and Pomeau in 1976 [11] and is also called the HPP model, a name derived from its inventors. Initially used for the description of the molecular dynamics of a classical lattice gas, the LGCA was later used to model large numbers of uniformly interacting particles (cells). Although LGCA has been used to model many physical systems [12], it has been used only in [13] to model self-organized avascular tumor in 2D. They simulated the LGCA model in only a 200×200 grid, a relatively small lattice for a 2D model. More information on their LGCA modeling approach is provided in their book [6]. However, the book only goes at length discussing biological pattern formation without offering the details of tumor growth modeling.

LGCA employs a regular, finite lattice and includes a finite set of particle states, an interaction neighborhood and local rules which determine the movement of particles (cells) and their transitions between states [6, 12, 14]. LGCA differ from traditional CA by incorporating the movement of particles and an exclusion principle. The particles in the model select from a finite number of permissible discrete velocity channels. The velocity specifies the direction and magnitude of movement, which may include zero velocity (rest). In a simple exclusion rule, only one particle may have each allowed velocity at each lattice site.

a

Number of Velocities	Velocities Available
1	
2	
3	
4	
5	

b

Velocity	s	l	r	u	d	Binary format
	1	0	0	0	0	10000
	0	0	1	0	0	00100
	0	1	0	0	0	01000
	0	0	0	1	0	00010
	0	0	0	0	1	00001
	0	1	1	0	0	01100
	0	1	0	1	1	01011
	0	1	1	1	1	01111

Fig. 1 (**a**) The number of velocities available in a node and their possible directions for a 2D LGCA. (**b**) Examples of binary representation of some possible velocities at a node in a 2D LGCA

Every node in the 2D LGCA model is associated with five velocity channels, namely *stay*, *left*, *right*, *up*, and *down*. Similarly, each node in a 3D LGCA model has seven velocity channels associated with it—*stay*, *left*, *right*, *up*, *down*, *front*, and *back*. For the case of a 2D LGCA model, the number of velocities and their possible directions are shown in Fig. 1a.

For a 2D LGCA model, the velocities associated with a particular node may be represented in binary format as shown in Fig. 1b. The notations *s*, *l*, *r*, *u*, and *d* in Fig. 1b represent *stay* (or rest), *left*, *right*, *up*, and *down*, respectively. The 3D LGCA model will have *f* and *b* representing *front* and *back*, respectively, in addition to the five velocities in the 2D LGCA model. For simulation purposes, binary representation means faster computation and smaller memory requirement, thus leading to the possibility of simulating a 3D tumor model.

3 Transition Rules

The transition rule of an LGCA has two steps [6, 14]. The first is an *interaction step* in which the state of each particle at each lattice site is updated. During this step, cells may appear (through reproduction) or disappear (through necrosis or

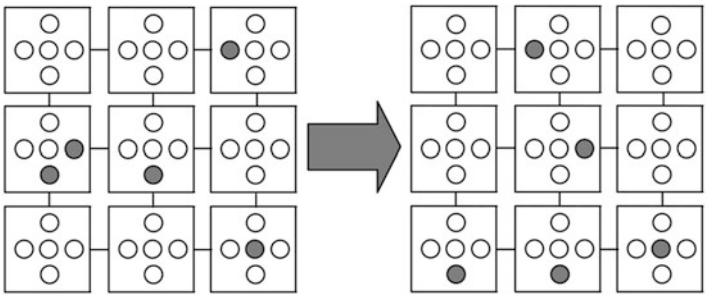

Fig. 2 Lattice configuration before (*left*) and after (*right*) the *transport step*. Particles have moved to the directions specified by the *gray dots*

apoptosis). Therefore, this step is neither number nor mass conserving. Moreover, the velocity state associated with each node in the lattice may change depending on the CA rule applied to them.

The second step is the *transport step* in which cells move synchronously in the direction and by the distance specified by their velocity state. The velocity state for each node in the lattice in a 2D LGCA model is represented in the five velocity channels inside the node (shown in Fig. 2 as five circles inside a node). The velocity state for each node in a 3D LGCA lattice is similarly represented in the seven velocity channels inside the node. This step is always number/mass conserving. An example of the lattice configuration before and after the *transport step* is shown in Fig. 2 for the case of a 2D LGCA model.

4 Formulation of the 3D LGCA Tumor Growth Model

We choose a cubic geometry for the 3D tumor lattice and the von-Neumann neighborhood with a radius of 1 as the interaction neighborhood. We employ a fixed boundary condition with normal cells present at the boundary at all times. As an initial condition, one cancer cell is seeded at the centre of the lattice.

The LGCA model incorporates a set of four states of cells for the four types of cells, namely normal, proliferating, quiescent, and necrotic cells.

For 3D simulation, we store data in a 3D matrix that consists of five layers of 2D matrices as shown in Fig. 3. The first and the second layers store the velocity states of the proliferating and necrotic cells, respectively, whereas the third and the fourth layers store the number of cancer and necrotic cells, respectively, in the von-Neumann neighborhood of each node (x, y, z). The fifth layer stores the information in the von-Neumann neighborhood of a node (x, y, z), i.e., information in cells at positions (x, y, z), $(x + 1, y, z)$, $(x-1, y, z)$, $(x, y + 1, z)$, $(x, y-1, z)$, $(x, y, z + 1)$, and $(x, y, z-1)$ and is used for imaging purposes.

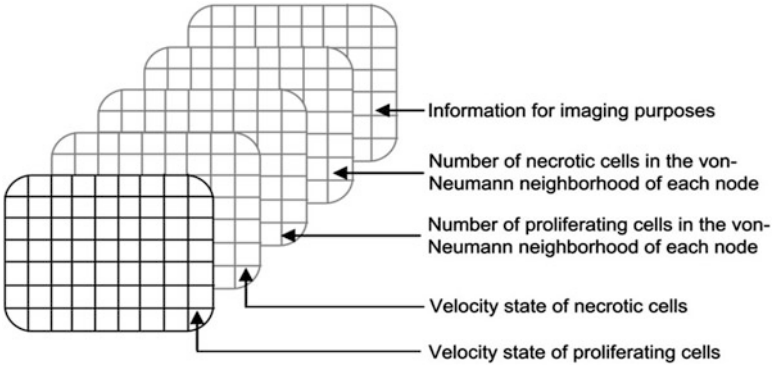

Fig. 3 Layers of the 3D matrix used to store data for the 3D tumor growth simulation

4.1 Interaction Step

As stated earlier, the first of the transition rules in the LGCA tumor growth model is an *interaction step* in which the state of each cell at each lattice site is updated. Unlike in the case of pure cellular automaton model coupled with oxygen diffusion equation [3], the fate of a cell in the case of the LGCA model is decided probabilistically by *Lattice–Boltzmann Energies*. We calculate the Lattice–Boltzmann energy for the tumor growth model using three parameters—K_{C-C}, K_{C-N} and K_{N-N} which are the *coupling coefficients* between cancer–cancer, cancer–necrotic, and necrotic–necrotic cells, respectively. The Lattice–Boltzmann energies for proliferation (E_p), quiescence (E_q), and necrosis (E_n) are given by Eqs. 1–3, respectively [15–17].

$$E_p = -\left[0.5\left\{C\left(C+1\right)K_{c-c} + N\left(N-1\right)K_{n-n}\right\} + \left(C+1\right)N\ K_{c-n}\right] \quad (1)$$

$$E_p = -\left[0.5\left\{C\left(C+1\right)K_{c-c} + N\left(N-1\right)K_{n-n}\right\} + \left(C+1\right)N\ K_{c-n}\right] \quad (2)$$

$$E_n = -\left[\begin{array}{l} 0.5\left\{\left(C-2\right)\left(C-1\right)K_{c-c} + N\left(N+1\right)K_{n-n}\right\} \\ +\left(C-1\right)\left(N+1\right)K_{c-n} \end{array}\right], \quad (3)$$

where, C, number of cancer cells in the interaction neighborhood; N, number of necrotic cells in the interaction neighborhood; K_{c-c}, coupling coefficient between cancer–cancer cells; K_{c-n}, coupling coefficient between cancer–necrotic cells; K_{n-n}, coupling coefficient between necrotic–necrotic cells.

The Lattice–Boltzmann energies calculated using Eqs. 1–3 are used to calculate the probabilities of proliferation, quiescence, and necrosis by using Eqs. 4–6, respectively.

$$P_{proliferation} = \frac{e^{E_p}}{e^{E_p} + e^{E_q} + e^{E_n}} \tag{4}$$

$$P_{quiescence} = \frac{e^{E_q}}{e^{E_p} + e^{E_q} + e^{E_n}} \tag{5}$$

$$P_{necrosis} = \frac{e^{E_n}}{e^{E_p} + e^{E_q} + e^{E_n}}, \tag{6}$$

where, $P_{proliferation}$, probability of proliferation; $P_{quiescence}$, probability of quiescence; $P_{necrosis}$, probability of necrosis.

4.2 Transport Step

In the *transport step*, the second step in the transition rules, cells move synchronously in the direction and by the distance specified by their velocity state. The velocity state is determined by two factors [6, 13]:

1. *The path of least resistance*: Cancer cells choose the path of least resistance to proliferate to, and hence, after cell division, the daughter cell moves to the node with the least density of cancer cells. We model this by determining the density of cancer cells in its neighborhood and changing the velocity state of the node such that the velocity points to the node that is the least dense.
2. *Chemotaxicity*: Necrotic cells produce chemotactic signals that tend to bind the necrotic cells together by attracting necrotic cells in the neighborhood. To model this phenomenon, we record the count of necrotic cells in the neighborhood of each node. The velocity state of the node containing the necrotic cell is then changed such that the velocity points to the direction of the node that contains the least number of necrotic cells.

After the velocity states at each node are determined, cells are transported synchronously in the directions specified by their velocity states.

5 Results and Discussion

We simulated the 3D LGCA tumor growth model on a desktop computer with a 3.2 GHz processor and 12 GB of RAM. We chose a lattice size of $200 \times 200 \times 200$ to simulate the tumor model so that the lattice remained sufficiently large and did

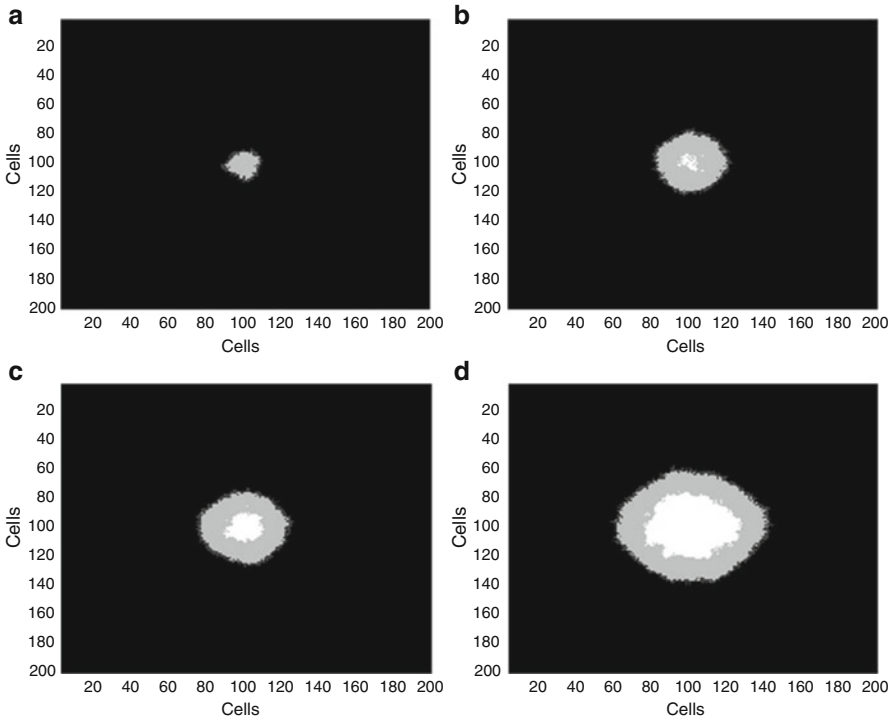

Fig. 4 The tumor after (**a**) 20, (**b**) 40, (**c**) 50, and (**d**) 90 time-steps during the growth simulation of the 3D LGCA tumor model

not influence the geometry of the tumor during growth. The simulation could be run for about 90 time-steps. The simulation could not progress further due to the unavailability of memory.

Figure 4 shows the tumor after (a) 20, (b) 40, (c) 50, and (d) 90 time-steps during the growth simulation of the 3D LGCA model. It is seen that during the initial growth stages, a core of quiescent cells (grey) appears at the centre of tumor surrounded by a rim of proliferating cells (Fig. 4a). Further growth progression leads to the appearance of a necrotic core (white) containing dead cells inside the tumor volume (Figs. 4 and 5b–d). This is similar to our earlier findings [2, 3] where we modeled tumor growth by employing the pure cellular automaton approach that was coupled with the solution to the oxygen concentration inside the tumor volume (Fig. 5a–d).

Figure 6 shows the cross-section of a growing tumor at depths of 22, 45, and 67 cells from the boundary. Once again, it is seen that the necrotic core (white) lies at the centre of the tumor and is encapsulated by quiescent cells (grey). The quiescent cells are similarly encapsulated by proliferating cancer cells that appear in the boundary of the tumor.

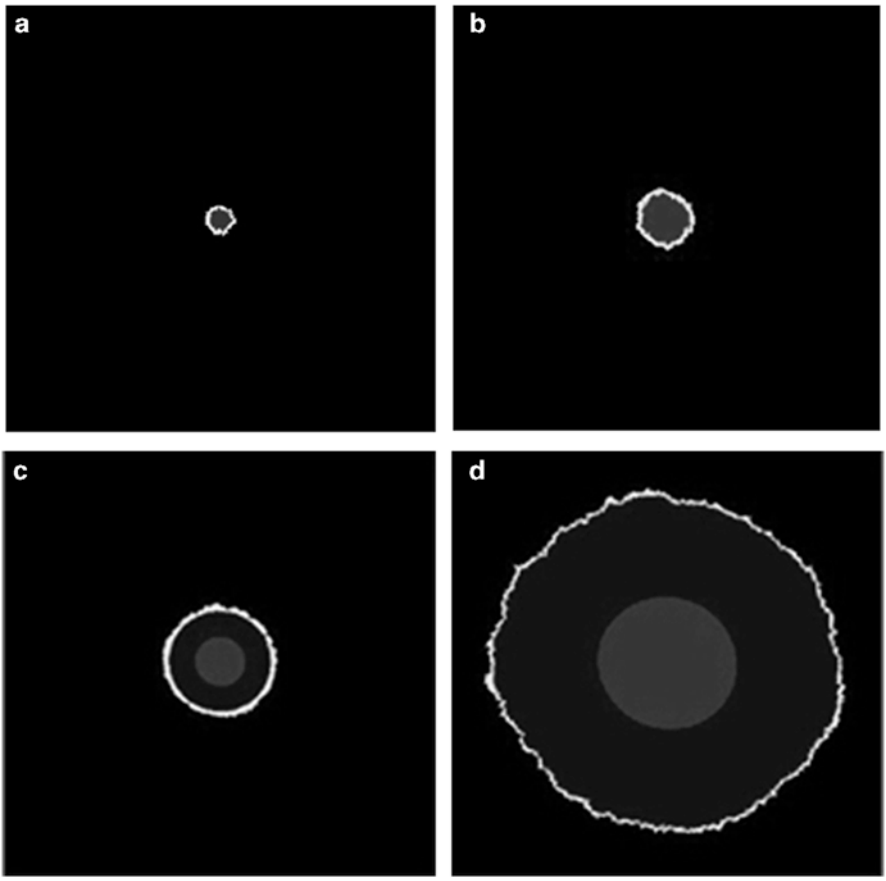

Fig. 5 Tumor at various stages of growth for the 2D CA model

To view the tumor in 3D, we imported the results in *3D Slicer* [18–20]. 3D Slicer is an open software platform developed for the analysis of 3D images especially for medical data. All image data obtained from the simulation of the LGCA tumor growth model need to be formatted to the *DICOM* (Digital Imaging and Communications in Medicine) standard [21] prior to being exported to 3D Slicer. Figure 7 shows the tumor in 3D at two different stages during the period of its growth after being imported in 3D Slicer.

Although a quantitative study of the results could not be made due to the unavailability of experimental data, as such data are generally the property of pharmaceutical companies funding the trial, the qualitative findings here lead us to believe that a detailed simulation and study of 3D tumor growth may be conducted by following this approach.

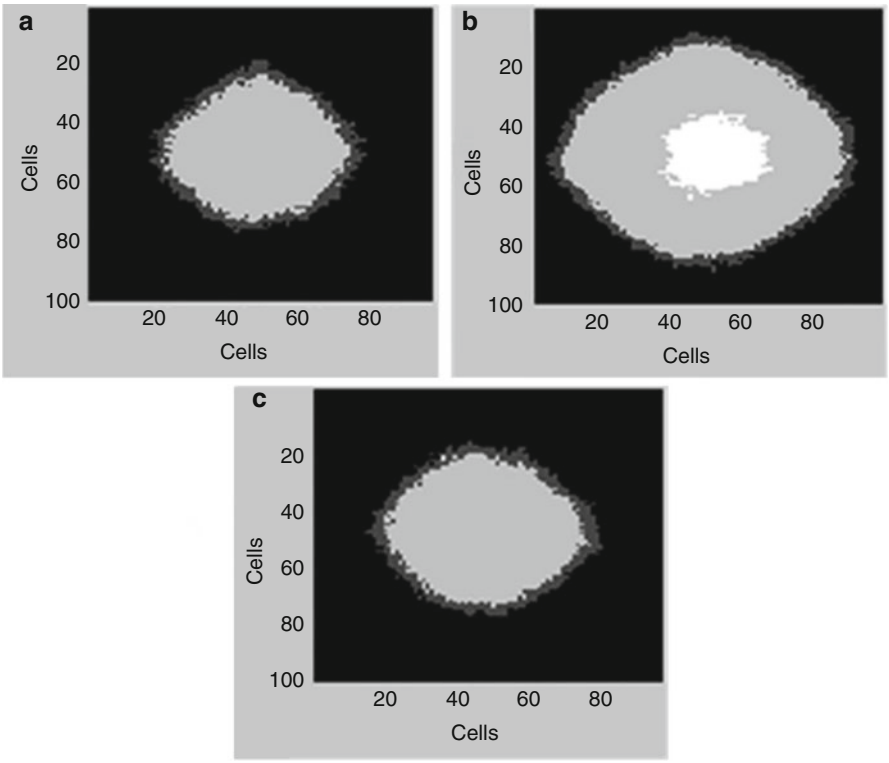

Fig. 6 The cross-sections of a growing tumor at depths of (**a**) 22, (**b**) 45, and (**c**) 67 cells from the boundary

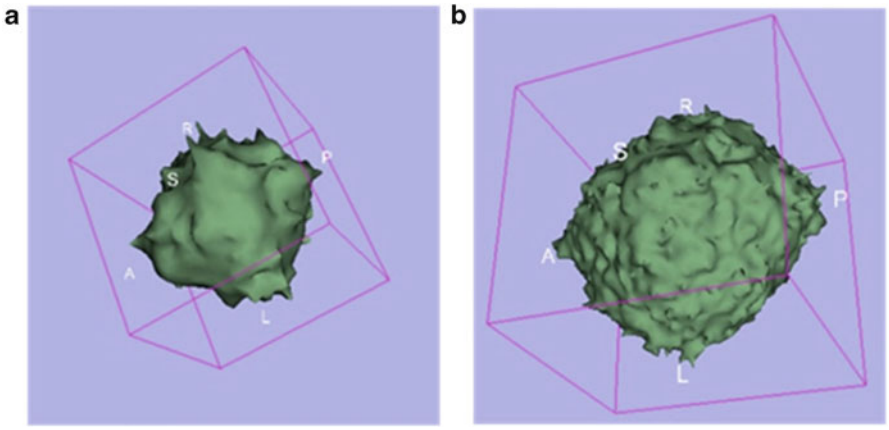

Fig. 7 The 3D view of the tumor, after being imported in 3D Slicer, at two different growth stages

Acknowledgements The first author was a SIRF scholar in Australia and was in receipt of the UIS scholarship during the completion of this research. The financial support of the National Health and Medical Research Council (Australia) Grant No. 1006031 is gratefully acknowledged.

References

1. Wolfgang A (2007) Molecular biology of human cancers. Springer, Dordrecht
2. Shrestha SMB, Joldes G, Wittek A, Miller K (2012) Modeling heterogeneous tumor growth using hybrid cellular automata. In: Nielsen PMF, Wittek A, Miller K (eds) Computational biomechanics for medicine. Springer, New York, pp 129–139
3. Shrestha SMB, Joldes GR, Wittek A, Miller K (2013) Cellular automata coupled with steady-state nutrient solution permit simulation of large-scale growth of tumours. Int J Numer Meth Biomed Eng 29(4):542–559
4. Qi A-S, Zheng X, Du C-Y, An B-S (1993) A cellular automaton model of cancerous growth. J Theoret Biol 161(1):1–12
5. Vermeulen L, Todaro M, de Sousa MF, Sprick M, Kemper K, Alea MP, Richel D, Stassi G, Medema J (2008) Single-cell cloning of colon cancer stem cells reveals a multi-lineage differentiation capacity. Proc Natl Acad Sci 105(36):13427–13432
6. Deutsch A, Dormann S, Maini PK (2005) Cellular automaton modeling of biological pattern formation: characterization, applications, and analysis. Springer, Berlin
7. Kansal A, Torquato S, Harsh G, Chiocca E, Deisboeck T (2000) Simulated brain tumor growth dynamics using a three-dimensional cellular automaton. J Theoret Biol 203(4):367–382
8. Sciumè G (2013) A multiphase model for three-dimensional tumor growth. New J Phys 15(1):015005
9. Frieboes HB, Jin F, Chuang Y-L, Wise SM, Lowengrub JS, Cristini V (2010) Three-dimensional multispecies nonlinear tumor growth—II: tumor invasion and angiogenesis. J Theoret Biol 264(4):1254–1278
10. Potts RB (1952) Some generalized order–disorder transformations. In: Proceedings of the Cambridge Philosophical Society. Cambridge University Press, Cambridge
11. Hardy J, De Pazzis O, Pomeau Y (1976) Molecular dynamics of a classical lattice gas: transport properties and time correlation functions. Phys Rev A 13(5):1949
12. Chopard B, Droz M (1998) Cellular automata modeling of physical systems, vol 122. Cambridge University Press, Cambridge
13. Dormann S, Deutsch A (2002) Modeling of self-organized avascular tumor growth with a hybrid cellular automaton. In Silico Biol 2(3):393–406
14. Weimar JR (1997) Simulation with cellular automata. Logos, Berlin
15. Rubenstein BM, Kaufman LJ (2008) The role of extracellular matrix in glioma invasion: a cellular potts model approach. Biophys J 95(12):5661–5680
16. Graner F, Glazier JA (1992) Simulation of biological cell sorting using a two-dimensional extended potts model. Phys Rev Lett 69(13):2013–2016
17. Wu FY (1982) The potts model. Rev Mod Phys 54(1):235
18. Gering D, Nabavi A, Kikinis R, Grimson WE, Hata N, Everett P, Jolesz F, Wells W (1999) An integrated visualization system for surgical planning and guidance using image fusion and interventional imaging. In: Taylor C, Colchester A (eds) Medical image computing and computer-assisted intervention. Springer, Berlin, Heidelberg, pp 809–819
19. Gering DT, Nabavi A, Kikinis R, Hata N, O'Donnell LJ, Grimson WEL, Jolesz FA, Black PM, Wells WM (2001) An integrated visualization system for surgical planning and guidance using image fusion and an open MR. J Magn Res Imag 13(6):967–975

20. Pieper S, Lorensen B, Schroeder W, Kikinis R (2006) The na-mic kit: Itk, vtk, pipelines, grids and 3d slicer as an open platform for the medical image computing community. In: 3rd IEEE International Symposium on Biomedical Imaging: Nano to Macro
21. Mildenberger P, Eichelberg M, Martin E (2002) Introduction to the dicom standard. European Radiol 12(4):920–927

http://www.springer.com/978-1-4939-0744-1

Computational Biomechanics for Medicine
Fundamental Science and Patient-specific Applications
Doyle, B.; Miller, K.; Wittek, A.; Nielsen, P.M.F. (Eds.)
2014, VIII, 122 p. 58 illus., 41 illus. in color., Hardcover
ISBN: 978-1-4939-0744-1